Appl. Phys. B 71, 611–615 (2000) / Digital Object Identifier (DOI) 10.1007/s003400000448

Applied Physics B
Lasers
and Optics

Rapid communication

Droplet velocity and acceleration measurements in dense sprays by laser flow tagging

S. Krüger, G. Grünefeld*

University of Bielefeld, Faculty of Physics, Postfach 100131, 33501 Bielefeld, Germany
(Fax: +49-521/1062-958, E-mail: gruenefe@physik.uni-bielefeld.de)

Received: 5 June 2000/Revised version: 28 July 2000/Published online: 6 September 2000 –

Abstract. The feasibility of liquid-phase velocity measurements in dense sprays by 2D laser-based flow tagging is demonstrated. Velocity measurements in dense sprays are difficult with conventional techniques because of the high number densities of droplets, the optical thickness of the medium, and multiple light-scattering effects. The present flow-tagging technique is based on phosphorescent tracer molecules, which are excited by a grid of pulsed 'write' laser beams. The motion of the tagged droplet groups can be observed by a CCD camera in this way. In addition, multiple consecutive velocity measurements are performed by 'droplet-group tracking'. This yields the acceleration along the trajectory of individual groups of droplets in unsteady sprays.

PACS: 47.27.-i; 42.62.Fi; 47.55.Kf

Well-established laser techniques such as phase Doppler anemometry (PDA) and particle-image velocimetry (PIV) are frequently used to measure spatially and temporally resolved droplet velocities in sprays [1]. However, severe difficulties are encountered when these techniques are applied to dense sprays. PDA suffers from high number densities of droplets and beam steering in high-temperature environments [2]. PIV is not applicable when the spray is so dense that the detected signal is strongly affected by multiple light scattering [3]. PIV requires that individual particles are resolved, and this becomes impossible when strong multiple scattering results in considerable image blurring. In addition, PIV suffers from strong out-of-plane motion, for example, in swirling sprays.

It should be noted that dense sprays are technically important. For example, high-pressure swirl injectors, generating dense hollow-cone sprays, are currently being developed for automotive direct-injection spark-ignition engines [4, 5].

It is demonstrated in the present study that droplet-velocity-field measurements can be performed in such dense sprays by laser-based flow tagging. Previous flow-tagging techniques are discussed elsewhere [6–13]. Most of these techniques require two laser pulses, i.e., 'write' and 'read' laser pulses, because they are based either on formation of tracer molecules by photodissociation, destruction of fluorescent parent molecules by photodissociation ('bleaching'), or molecular pump and probe mechanisms [6–11]. In contrast, flow tagging can also be performed by a single laser pulse when phosphorescent substances are used as the tracer [12, 13]. These techniques are therefore particularly attractive. The spatial position of the laser-excited phosphorescent substances is recorded by a gated camera after being convected by the flow. The use of phosphorescent substances also allows the performance of multiple consecutive velocity measurements within the phosphorescence lifetime. Thus, the trajectory and acceleration of fluid elements can be determined. This yields additional information, in particular in unreproducible, turbulent flows. It is demonstrated in this paper that 'droplet-group tracking' can be done in this way.

It was mentioned above that PDA and PIV encounter severe problems in dense sprays. In contrast, a laser flow-tagging technique is hardly affected by multiple light scattering when the distance and width of the tag lines are wide enough, so that they can still be resolved. Beam attenuation does not affect the feasibility of the technique, as long as the tag lines are recognized. Laser-beam steering is not an important factor because the spatial positions of the 'write' laser beams can be recorded. Therefore, laser flow tagging can be performed in dense sprays. This was demonstrated previously, when the velocity field of the gas phase was measured in a dense spray [11]. It should also be noted that strong out-of-plane motion is not problematic in most flow-tagging experiments. Thus, it is possible to do the measurements, for example, in dense swirling sprays. It is also noteworthy that the three velocity components in a plane can be measured by stereoscopic flow tagging [10].

1 Experimental

Initial measurements have been performed in a hollow-cone gasoline direct-injection spray. The prototype swirl injector and electronics were supplied by S. Arndt (Robert Bosch

*Corresponding author.

GmbH, Stuttgart). It has been operated with 50 bar rail pressure in room air. Ethanol has been used as the fuel. The measurements have been performed at 1 ms after triggering the injector, i.e., in the fully developed spray pulse (pulse length: 1.5 ms) The maximum droplet density is about 5×10^6 /cm^3 in the probe volume. The Sauter mean diameter of the droplets is $d_{32} \sim 15\,\mu$m [14] (thus, the average droplet spacing at maximum density is $\sim 4d_{32}$). This spray is comparable to previously investigated sprays, in which PIV measurements proved to be difficult [3].

The flow-tagging set-up is outlined in Fig. 1, but the detector is not shown. An image-intensified double-frame 'progressive scan' CCD camera (PCO Sensicam) is employed as the detector. It is capable of recording two images with a delay down to $\sim 1\,\mu$s. The gated image intensifier also acts as a shutter in front of the recording system with a minimum gate length of ~ 100 ns. It is clear that the gate length determines the extent to which a phosphorescence image is blurred during the exposure time.

A Mie scattering image that has been recorded with a thin laser sheet in the central plane of the spray is included in Fig. 1 to demonstrate the field of view and the orientation of the spray. The field of view (33 mm × 44 mm) has been imaged onto the CCD camera at a right angle by using a spherical focussing mirror ($f = 35$ cm, $d = 25$ cm, aluminum).

The central region of the spray is illuminated by a 'write' laser grid as shown in Fig. 1. A frequency-quadrupled (266-nm) Nd:YAG laser (Spectra Physics) is used as the laser source. Two sets of 'write' laser lines, each ~ 1 mm × 2 mm in diameter ($\sim 70\,\mu$J/pulse), are created by splitting and focussing the beam of the Nd:YAG laser (Spectra Physics), basically by using two arrays of 15 cylindrical lenses ($f = 30$ cm).

Flow tagging is performed in this work by using phosphorescent molecules as mentioned in the introduction. A lanthanide chelate (Tb^{3+}-dipicolinic acid, Molecular Probes) dissolved in ethanol (10^{-3} M) is employed in the present experiment. Lanthanide chelates are frequently used for time-resolved luminescence measurements, for example, in biology [15, 16]. The lifetime of the terbium chelate is roughly 1 ms. It exhibits a broad absorption peak around 280 nm. The phosphorescence occurs at two sharp peaks at 491 nm and 545 nm [16], which are both collected by the camera system.

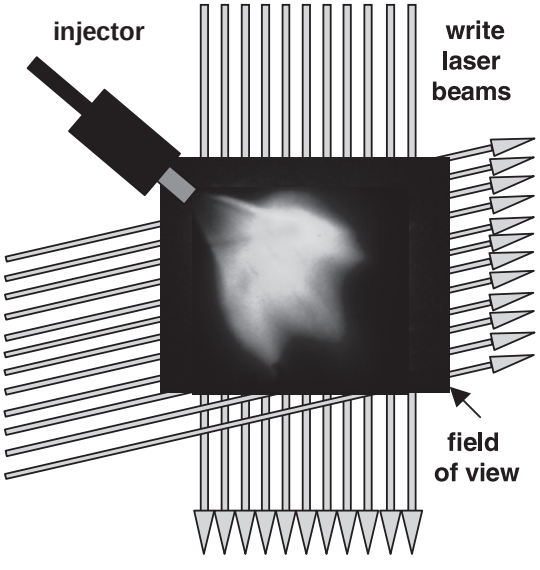

Fig. 1. Experimental set-up. The intensified CCD camera is not shown. Instead, a Mie scattering image is included showing the spray at 1 ms after triggering the injector. Only the first vertical write-laser beam on the left-hand side is used for the acceleration measurements

Biacetyl is another interesting phosphorescent molecule that may be used for flow-tagging measurements in sprays [13]. However, there are at least two drawbacks compared to lanthanide chelates. First, phosphorescence from biacetyl is easily quenched by oxygen. Thus, the medium must be free of oxygen. Secondly, some of the biacetyl may leave the droplets in the spray due to its high vapor pressure. Thus, some of the phosphorescence may arise from the gas phase and, consequently, there might be cross-talk with the velocity of the gas phase (this problem may be overcome by exploiting phosphorescence quenching by oxygen in the gas phase).

It was mentioned in the introduction that the instantaneous position of the 'write' laser lines must be measured in the spray if they are affected by beam steering. This can be done by recording laser-induced emissions (phosphorescence or elastic scattering) at $t \approx 0$. It is clear that this calibration image must be acquired in each individual measurement if beam steering fluctuates from pulse to pulse. The double-frame camera mentioned above has been used for this purpose. However, it can be assumed that the position of the laser beams in the spray is reproducible from pulse to pulse in most applications (compare [11]). Thus, it is also possible to record the calibration image once in advance. Consequently the double-frame option of the camera could be used for instantaneous acceleration-field measurements by recording two images at $t_1 > 0$ and $t_2 > t_1$.

However, the trajectory and acceleration of individual droplet groups is measured by acquisition of a series of phosphorescence images in a single frame using the gated image intensifier in the present work ('droplet-group tracking'). Only one of the write-laser beams shown in Fig. 1 is used in that experiment in order to avoid overlap of the phosphorescence signals from neighboring beams in the image.

2 Results and discussion

Figure 2 shows a pair of typical phosphorescence single-shot images measured in the spray with a delay of $\Delta t = 15\,\mu$s. Both images have been measured in an individual spray pulse using the double-frame camera described above. There is no residual Mie scattering in these images because both have been recorded after the laser pulse. Figure 2a has been measured at 1–6 μs after the laser pulse, and Fig. 2b has been measured at 16–21 μs after the laser pulse (gate length: 5 μs). The hollow-cone structure of the spray can be nicely seen in these images. The phosphorescence signal-to-noise ratio is very high (> 100) in the droplet mainstream, i.e., close to the edge of the spray cone. In contrast, the signal-to-noise ratio is poor in some regions around the spray axis, in particular close to the nozzle, due to low droplet density.

The displacement field of the distorted grid in Fig. 2b with regard to the initial grid in Fig. 2a yields the instantaneous droplet-velocity field. The displacement field is found by employing an optical flow algorithm [17]. The resulting instanta-

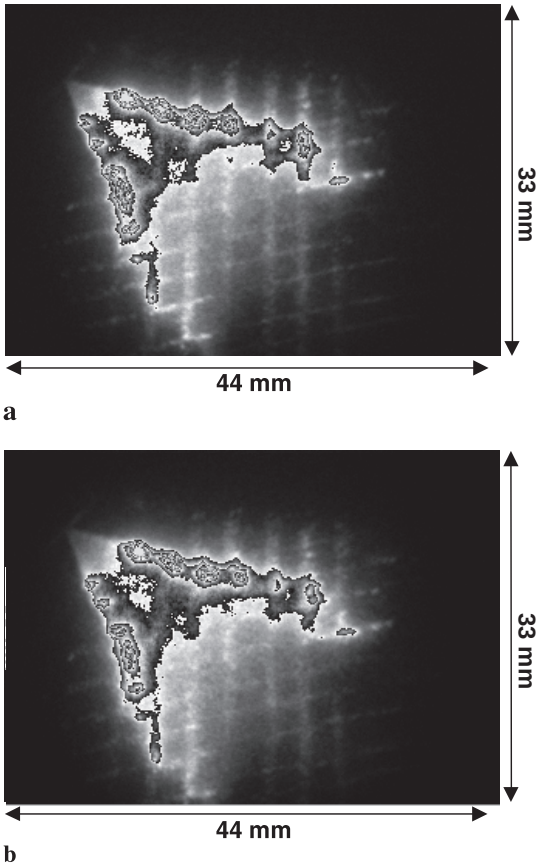

Fig. 2. Pair of phosphorescence single-shot images recorded in a single spray pulse with a delay of $\Delta t = 15\,\mu s$

neous velocity field is given in Fig. 3. One of the 'branches' of the droplet mainstream is indicated by a straight line in Fig. 3. The velocity-magnitude profile along this line is plotted in Fig. 4. The maximum drop velocity found in the mainstream is $\sim 90\,m/s$. Much smaller drop velocities are found in the inner region of the spray where the droplet density is low. This can be explained by the fact that the droplets in the inner region of the spray are generally smaller than those in the mainstream, because they follow the entrainment air flow more easily [4, 11]. It is clear that smaller droplets are decelerated more rapidly than larger droplets.

The instantaneous velocity field was found to be quite reproducible from pulse to pulse. In particular, the standard deviation of the instantaneous velocity measurements in the droplet mainstream is in the range 5%–10%. It can be seen in Fig. 4 that the velocity-magnitude profiles in the mainstream of an instantaneous and an averaged measurement are indeed very similar, in particular close to the nozzle. This implies that the relative error of the instantaneous measurements is also smaller than 5%–10%, at least in these regions with high signal-to-noise ratio. The mean velocity and standard-deviation fields will be discussed in more detail in a forthcoming paper. The spatial resolution of this technique will also be discussed in a forthcoming paper. Briefly, the resolution is at least half the spacing of the tag lines, i.e. $\sim 1.6\,mm$ in the present application.

The velocity distribution in the droplet mainstream is not as uniform or smooth as one might expect. This can be seen in particular in Fig. 4. There are a number of significant and reproducible velocity peaks and valleys in the droplet mainstream. Most of these structures are clearly resolved, since they are larger than the spatial resolution of $\sim 1.6\,mm$. However, the appearance of these structures does not imply that the droplets were accelerated in some regions when they travel in the mainstream. Instead, it will be demonstrated in the following that this velocity distribution is caused by unsteady effects.

It was mentioned above that 'droplet-group tracking' can be performed by a series of instantaneous velocity measurements within the lifetime of the phosphorescent tracer. A typical unprocessed CCD image is given in Fig. 5. It results from 10 exposures ($\Delta t = 40\,\mu s$, gate length $= 3\,\mu s$) after a single laser pulse. Only one of the write-laser beams is used in this experiment, which is indicated in Fig. 5. A well-defined group of droplets in the upper branch in the droplet mainstream is illuminated by this laser beam. The vertical extension of the droplet group is limited by the dimension of the droplet distribution in the upper mainstream. This results in a number of well-resolved phosphorescence spots in the image in Fig. 5. It can be seen in the image that the illuminated droplet group in the lower branch is not as well defined

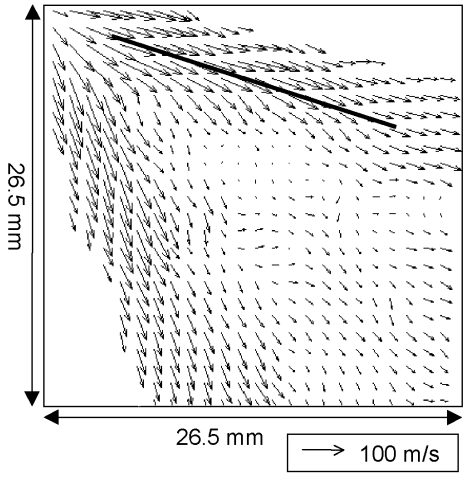

Fig. 3. Instantaneous droplet-velocity field resulting from the image pair in Fig. 2

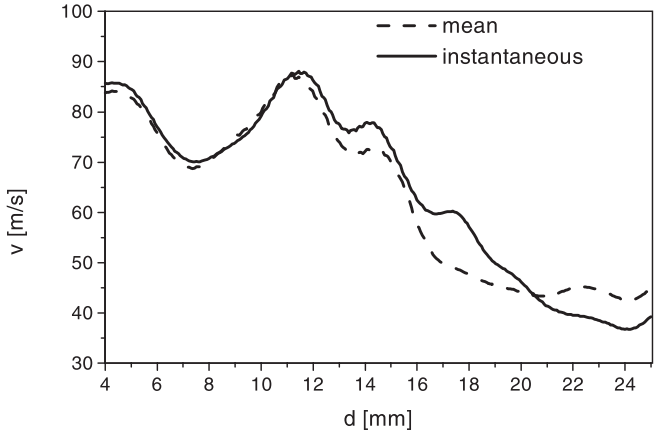

Fig. 4. Velocity-magnitude profile along the straight line in Fig. 3 (d is the distance from the nozzle). An instantaneous measurement and the average of 20 instantaneous measurements are given

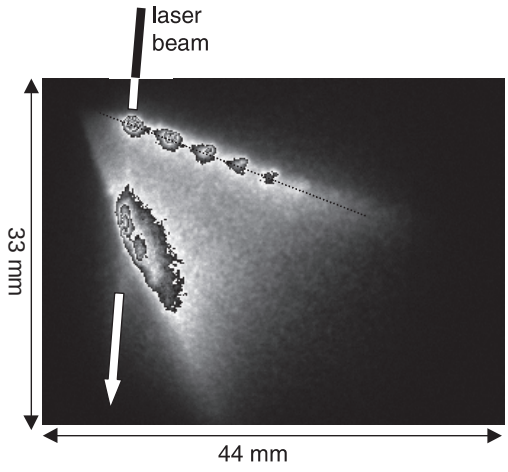

Fig. 5. 'Droplet-group tracking': unprocessed multi-exposure image measured after a single laser pulse using a single laser beam ($\Delta t = 40\,\mu s$)

due to an unfavorable angle of the laser beam with regard to the lower mainstream. Thus, only the upper branch is considered in the following.

Measured images like Fig. 5 turned out to be quite reproducible. A corresponding profile from an image averaged over 10 measurements is also given in Fig. 6. It can be seen that it is quite similar to the 'instantaneous' measurement, although the phosphorescence spots are blurred.

It is clear that the position of the phosphorescence spots and their spacing represent the trajectory and instantaneous velocities of the illuminated droplet group. It can be observed in Fig. 5 that the trajectory can be approximated by a straight line (dotted line). An image-intensity profile along this line ('d axis') is plotted in Fig. 6. At least six phosphorescence spots can be seen in Figs. 5 and 6. The intensity of these spots decreases from left to right, basically because of the dispersion of the droplet group (see below) and due to the phosphorescence decay. It can also be seen in Fig. 5 that these spots are sitting on a broad background (~ 200 arbitrary units, compare Fig. 6) that arises basically from multiple light scattering.

The first six phosphorescence spots in Fig. 6 yield five consecutive velocity measurements, which are plotted in Fig. 7. The accuracy of these measurements can be estimated to be $\sim 5\%$ on the average, based on the displacements and the uncertainty to determine the center of the phosphorescence spots [11] (Fig. 6 shows clearly that the error of the measurements closer to the nozzle is smaller than the error of the measurements further downstream). The data in Fig. 7 show that the deceleration, a, is uniform (within the measurement uncertainty) across the field of view ($a = -1.4 \times 10^5\,\mathrm{m/s^2}$). It should be noted that this velocity profile is significantly different to the instantaneous profile in Fig. 4, which has been determined in the same region. Consequently, the large 'oscillations' of the velocity found in the instantaneous (and mean) velocity fields, in particular close to the nozzle, are due to unsteady spray behavior. This means that the droplet velocity field within each spray pulse is time-dependent, for example due to variations in the fuel flow through the nozzle. However, these variations are found to be quite reproducible from pulse to pulse as seen in Fig. 4.

The 'droplet-group tracking' measurements also yield information on the dispersion of individual droplet groups. The extension of the droplet group is approximately given by the width (FWHM) of the phosphorescence spots. The measure-

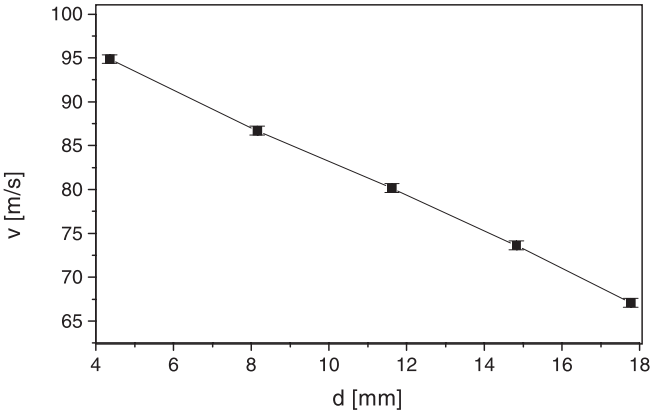

Fig. 7. Five consecutive velocity measurements resulting from Fig. 5 and the 'instantaneous' image-intensity profile in Fig. 6

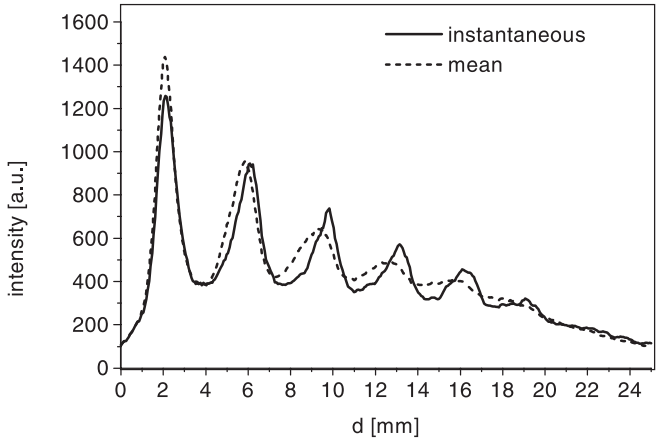

Fig. 6. Unprocessed image-intensity profile along the dotted line in Fig. 5 ('instantaneous') and corresponding profile from an image averaged over 10 measurements ('mean'); d is the distance from the nozzle

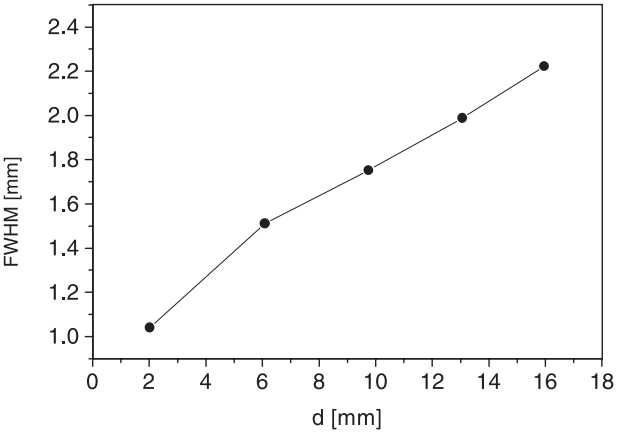

Fig. 8. Width of consecutive phosphorescence spots as a function of d (distance from the nozzle). The data are averaged over 20 'single-shot' measurements (compare Fig. 5)

ment shown in Fig. 5 has been repeated 20 times and the data have been averaged over this ensemble in order to reduce the noise. The resulting FWHM (in the direction of the d axis) is given in Fig. 8. It can be seen that the width of the droplet groups increases continuously by a factor of ~ 2 over a distance of 14 mm. Such information can be used to study the droplet–gas and droplet–droplet interactions in the spray.

3 Summary and conclusions

It is demonstrated that instantaneous droplet-velocity fields can be measured in dense sprays by the present flow-tagging method. In comparison to well-established techniques, such as PDA and PIV, the present technique is much less affected by multiple light scattering, beam steering and beam attenuation in optically thick two-phase flows.

The flow-tagging technique based on a phosphorescent tracer can in principle be performed by a single laser source and a single-frame camera. It is noteworthy that the technical effort of typical double-pulsed PIV measurements is higher.

Furthermore, it is demonstrated that the trajectory and acceleration of individual droplet groups can be determined by a number of consecutive velocity measurements. This yields additional information on the dynamic motion of the droplets and the interaction with the gas phase. The latter can be studied more thoroughly by combining the present technique with the gas-phase velocimetry method proposed previously [11].

We also did flow-tagging measurements in the dense spray close to a wall in order to investigate spray–wall interaction. Such results will be presented in a forthcoming paper.

Acknowledgements. This work has been supported by the German Federal Ministry for Science and Education (BMBF) under contract No. 13N7182/1. The authors are also grateful to Dr.S. Arndt, Robert Bosch GmbH, Stuttgart, Germany, for providing the injector and for some stimulating discussions.

References

1. W.D. Bachalo: Int. J. Multiphase Flow **20**(Suppl.), 261 (1994); A. Brandt, W. Merzkirch: Part. Part. Syst. Charact. **11**, 1568 (1994)
2. J.-F. Le Coz: In Ninth International Symposium on Applications of Laser Techniques to Fluid Mechanics, Paper 7.3, Lisbon, Portugal (1998); L. Araneo, C. Tropea: In Spray '99, 5. Workshop über Techniken der Fluidzerstäubung und Untersuchungen von Sprühvorgängen, Universität Bremen (1999) [in English]
3. W. Hentschel, A. Homburg, G. Ohmstede, T. Müller, G. Grünefeld: SAE Tech. Paper No. 1999-01-3660 (1999)
4. F. Zhao, M.-C. Lai, D.L. Harrington: Prog. Energy Combust. Sci. **25**, 437 (1999)
5. G.K. Fraidl, W.F. Piock, M. Wirth: SAE Tech. Paper No. 960465 (1996)
6. J.A. Wehrmeyer, L.A. Ribarov, D.A. Oguss, F. Batliwala, R.W. Pitz: AIAA Paper 99-0646, 37th Aerospace Sciences Meeting & Exhibit, Jan. 11–14, Reno, NV (1999); L.A. Ribarov, J.A. Wehrmeyer, F. Batliwala, R.W. Pitz, P.A. DeBarber: AIAA J. **37**, 708 (1999)
7. R.B. Miles, D. Zhou, B. Zhang, W.R. Lempert: AIAA J. **31**, 447 (1993); R.B. Miles, C. Cohen, J. Connors, P. Howard, S. Huang, E. Markowitz, G. Russell: Opt. Lett. **12**, 861 (1987)
8. L.R. Boedecker: Opt. Lett. **14**, 473 (1989); C. Orlemann, C. Schulz, J. Wolfrum: Chem. Phys. Lett. **307**, 15 (1999)
9. H. Finke, G. Grünefeld: An experimental investigation of extinction of curved laminar hydrogen diffusion flames, In Proc. Combust. Inst. 28, Symposium (International) on Combustion, Edinburgh (2000)
10. S. Krüger, G. Grünefeld: Appl. Phys. B **69**, 509 (1999)
11. S. Krüger, G. Grünefeld: Appl. Phys. B **70**, 463 (2000)
12. R.E. Falco, C.C. Chu: Proc. SPIE **814**, 706 (1987)
13. B. Hiller, R.A. Booman, C. Hassa, R.K. Hanson: Rev. Sci. Instrum. **55**, 1964 (1984)
14. S. Arndt: Private Communication, Robert Bosch GmbH, Stuttgart, Germany (1999)
15. I. Hemmilä: J. Alloys Compd. **225**, 480 (1995)
16. E.F. Gudgin Dickson, A. Pollak, E.P. Diamandis: J. Photochem. Photobiol. B **27**, 3 (1995)
17. P.T. Tokumaru, P.E. Dimotakis: Exp. Fluids **19**, 1 (1995); G. Grünefeld, H. Finke, J. Bartelheimer, S. Krüger: Exp. Fluids, in press (1999)